

A time scale for electrical screening in pulsed gas discharges

Jannis Teunissen¹, Anbang Sun¹, Ute Ebert^{1,2}

¹Centrum Wiskunde & Informatica (CWI), P.O. Box 94079, 1090 GB Amsterdam, The Netherlands,

²Dept. Physics, Eindhoven Univ. Techn., The Netherlands,

E-mail: jannis@teunissen.net

Abstract. The Maxwell time is a typical time scale for the screening of an electric field in a medium with a given conductivity. We introduce a generalization of the Maxwell time that is valid for gas discharges: the *ionization screening time*, that takes the growth of the conductivity due to impact ionization into account. We present an analytic estimate for this time scale, assuming a planar geometry, and evaluate its accuracy by comparing with numerical simulations in 1D and 3D. We investigate the minimum plasma density required to prevent the growth of streamers with local field enhancement, and we discuss the effects of photoionization and electron detachment on ionization screening. Our results can help to understand the development of pulsed discharges, for example nanosecond pulsed discharges at atmospheric pressure or halo discharges in the lower ionosphere.

1. Introduction

When a weakly ionized plasma is exposed to an external electric field, charges will move to screen the plasma interior from the field. A typical time scale for this process is the Maxwell time, also known as the dielectric relaxation time [1], that depends on the mobility and density of charge carriers in the plasma. In this paper, we present a generalization of the Maxwell time that is also valid for electric fields above breakdown, by taking into account charge multiplication. We call this generalization the *ionization screening time*.

Our motivation for investigating electric screening in discharges came from two other articles [2, 3], in which we simulated the breakdown of ambient air. We included background ionization in the form of negative ions, from which electron avalanches could grow after electron detachment. These avalanches together started screening the electric field, but we could not simulate up to the end of this process. Therefore, we briefly introduced the concept of an *ionization screening time* in [2]. This name was inspired by a similar phenomenon: after a lightning stroke, ionization screening waves can form in the lower ionosphere, also known as halos [4].

In this paper, we investigate the ionization screening time in more detail. The paper is organized in the following way. In section 2 the Maxwell time is discussed and the ionization screening time is introduced. Our analytic estimate for the ionization screening time is compared with simulation results in section 3. These simulations are performed in 1D and 3D, using a fluid and a particle model. For low levels of initial ionization, discharges become inhomogeneous and local field enhancement becomes important, which is investigated in section 4. Finally, we discuss the effect of electron detachment and photoionization on the screening process in section 5, which is especially relevant for air.

2. The ionization screening time

Below, we first discuss the Maxwell time, also known as the dielectric relaxation time [1]. Then we introduce the ionization screening time, for which we give an analytic estimate.

2.1. The Maxwell Time

Although the Maxwell time is valid for any medium with a constant conductivity, we focus here on the case of a plasma. Suppose we have a neutral plasma with an electron density n_e on which an electric field \vec{E} is applied. The field accelerates the electrons in the plasma, while collisions slow them down again. This gives rise to an electrical current

$$\vec{J}_e = en_e\mu_e\vec{E}, \tag{1}$$

where μ_e denotes the electron mobility and e the elementary charge. (We ignore the much smaller contribution of the ions.) This current reduces the electric field inside the plasma. By taking the divergence of Ampère's law, we can relate the current to the time derivative of the electric field

$$\nabla \cdot (\vec{J}_e + \varepsilon_0 \partial_t \vec{E}) = 0, \quad (2)$$

where ε_0 is the dielectric permittivity. This equation can be interpreted more easily if we assume the system is planar, i.e., effectively one-dimensional, so that we get a scalar equation. If a constant external field E_0 (i.e., $\partial_t E_0 = 0$) is applied from some location outside the plasma, integration of (2) gives

$$\partial_t E = -J_e/\varepsilon_0 = -(en_e \mu_e/\varepsilon_0) E. \quad (3)$$

A typical time scale for electric screening is given by $-E/\partial_t E$, which is called the Maxwell time:

$$\tau_{\text{Maxwell}} = \varepsilon_0/(en_e \mu_e). \quad (4)$$

For a different derivation see [5]. Note that there is no dependence on the density profile at the plasma boundary.

2.2. The ionization screening time

When the field E_0 applied to a plasma is above the breakdown threshold, the Maxwell time is no longer valid, because the electron density n_e grows in time.

We present a generalization of the Maxwell time, which we call the *ionization screening time* or τ_{is} . It estimates how long it takes for the electric field inside a discharge to drop below the breakdown threshold. Below we present a derivation, the result of which is

$$\tau_{\text{is}} = \ln \left(1 + \frac{\alpha_{\text{eff}} \varepsilon_0 E_0}{en_0} \right) / (\alpha_{\text{eff}} \mu_e E_0), \quad (5)$$

where α_{eff} is the effective ionization coefficient. Note that in the limit $\alpha_{\text{eff}} \rightarrow 0$, equation (5) reduces to the Maxwell time (4).

2.3. Analytic estimate

To derive an analytic estimate for the ionization screening time, we study a simplified system. The assumptions are listed below:

- The system is planar (effectively one-dimensional); there is spatial variation in the x -direction only.
- Initially, the electron and ion density is n_0 between x_0 and x_1 , and zero elsewhere. The width $x_1 - x_0$ is taken larger than the distance the electrons will drift up to the ionization screening time.
- Electrons keep the same drift velocity $v_d = \mu_e E_0$ and effective ionization coefficient α_{eff} as in the initial background field E_0 .

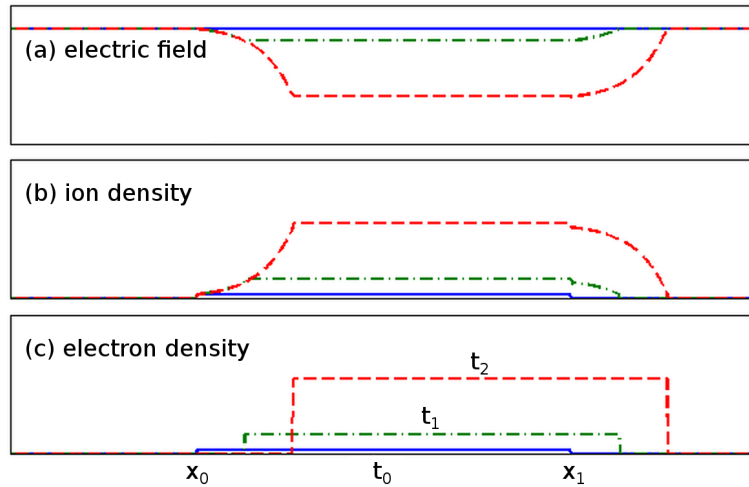


Figure 1. Schematic view of (a) electric field, (b) ion density and (c) electron density at three times $t_0 < t_1 < t_2$. The electric field decreases in the ionized region due to the charge separation at the left and right boundary.

- There is no diffusion.

The evolution of this system will resemble the one depicted in figure 1. The electrons, which are initially present between x_0 and x_1 , drift to the right with velocity v_d . Their number density grows in time as $e^{\alpha_{\text{eff}} v_d t}$. At time t there are no electrons below $x_0 + v_d t$, while they have created an ion density $n_0 e^{\alpha_{\text{eff}}(x-x_0)}$ between x_0 and $x_0 + v_d t$. Therefore, the integrated net charge in this region is $(e^{\alpha_{\text{eff}} v_d t} - 1)en_0/\alpha_{\text{eff}}$. Equating this to the charge $\varepsilon_0 E_0$ needed to screen an electric field E_0 , and solving for t gives the following expression for the ionization screening time

$$\tau_{\text{is}} = \ln \left(1 + \frac{\alpha_{\text{eff}} \varepsilon_0 E_0}{en_0} \right) / (\alpha_{\text{eff}} v_d), \quad (6)$$

where v_d can be replaced by $\mu_e E_0$.

In deriving equation (6) we have assumed that α_{eff} and v_d keep their values for the initial field E_0 . This approximation becomes more accurate if the initial electron density n_0 is small compared to the density at the time of screening. Then the electric field stays close to E_0 during most of the screening process, because the charge density is not yet large enough to affect it. Note that by using these initial coefficients we will underestimate the ionization screening time. This is somewhat compensated for by computing the time to shield the electric field to zero, instead of to a value below breakdown.

3. Comparison with simulations

We will now compare the predictions of equation (6) with numerical simulations. In these simulations, we determine how long it takes for the electric field inside a discharge to drop below the breakdown threshold. We perform these comparisons in nitrogen at

1 bar and 293 Kelvin, for which we have used a breakdown field of 3 MV/m. (Since there are no electron loss mechanisms in pure nitrogen, the breakdown field is not well-defined.) Below, we describe the simulation models.

3.1. Simulation Models

We use two types of simulation models here: a plasma fluid model (1D) and a particle model (1D and 3D). It will turn out that in 1D, the fluid model gives almost the same results as the particle model. We nevertheless include both, to provide a link between the 3D particle simulations presented in section 3.3 and the plasma fluid description used for equation (6).

In all cases, a spatial resolution of 8 μm and a time step of 1 ps was used. In 1D, the computational domain was 16 mm long. In 3D, the computational domain measured 8 mm along the x -direction, with an area of $1 \times 1 \text{ mm}^2$ in the transverse direction. To get the planar structure of the 1D simulations in 3D, we have used periodic boundary conditions in the transverse direction.

3.1.1. 1D fluid model The plasma fluid model that we use is of the drift-diffusion-reaction type [6]. It contains the following equations:

$$\partial_t n_e = \nabla \cdot (\mu_e \vec{E} n_e + D_e \nabla n_e) + \alpha_{\text{eff}} \mu_e |\vec{E}| n_e, \quad (7)$$

$$\partial_t n^+ = \alpha_{\text{eff}} \mu_e |\vec{E}| n_e, \quad (8)$$

$$\nabla \cdot \vec{E} = e(n^+ - n_e)/\epsilon_0, \quad (9)$$

where D_e is electron diffusion coefficient and n^+ is the density of positive ions. In the simulations, the coefficients μ_e , D_e and α_{eff} depend on the local electric field, which is recomputed at every time step. These coefficients are computed from the particle cross sections [7] by measuring the properties of simulated particle swarms, see [8]. The same coefficients are used for equation (6).

The fluid equations are solved with a third-order upwind scheme, as in [6]. Time stepping was done with the classic fourth order Runge-Kutta scheme.

3.1.2. 3D particle model The 3D model is of the PIC-MCC type, with electrons as particles and ions as densities. The electrons randomly collide with a background of neutral molecules. We use cross sections from the Siglo database [7], Fishpack [9] to compute the electric potential and adaptive particle management for the super-particles [10]. This model is described in some detail in [2, 3].

3.1.3. 1D particle model The 1D particle model was constructed from the 3D particle model described above. The 3D model is converted to 1D by projecting the particles onto one spatial dimension for the calculation of the electric field. The particles then have just one coordinate for their position, but their velocities still have three components.

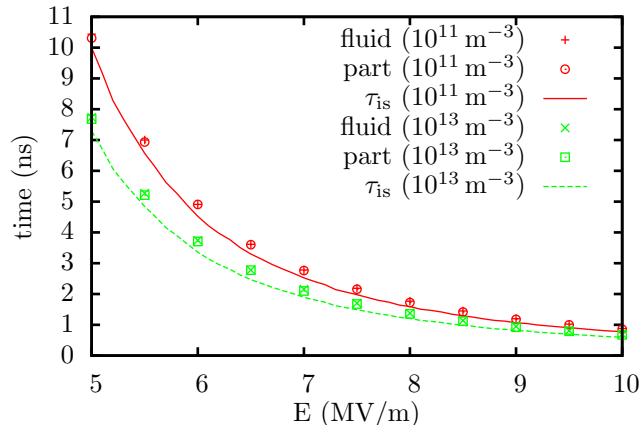


Figure 2. The ionization screening time versus the applied electric field, for two initial plasma densities (10^{11} and 10^{13}). Results are shown for a 1D fluid model, a 1D particle model and equation (6), for N_2 at 1 bar.

3.2. Comparison with 1D simulations

We now compare our analytic approximation to the two numerical simulation models. In figure 2, we show the screening time for fields between 5 and 10 MV/m. Two initial conditions are used: an electron and ion density of 10^{13} or 10^{11} m^{-3} was present between 12 and 14 mm. Equation (6) predicts shorter screening times than we see in the simulations, but the agreement is nevertheless quite good. Note that the particle and fluid model give almost identical results.

As discussed in section 2.3, the partial screening of the electric field was not included in deriving equation (6). An example of this partial screening is shown in figure 3, where the electric field and the electron density are shown at various times, using the 1D fluid model in a background field of 6 MV/m. Close to the screening time, the exponential growth of the electron density slows down, because the field is partially screened.

3.3. Comparison with 3D simulations

To investigate how inhomogeneities affect the ionization screening time, we have performed 3D particle simulations in a field of 6 MV/m.

We will show results using two initial plasma densities: 10^{13} and 10^{11} m^{-3} . In both cases, the plasma is initially present between 4 and 6 mm. Because the electric field is now a varying 3D vector field, we cannot directly compare it to the 1D results. Therefore, we show the electric field and the electron density averaged over transverse planes. This leaves only the longitudinal component of the field nonzero, due to the periodic boundary conditions.

We first present the results for an initial density of $n_0 = 10^{13} \text{ m}^{-3}$ between 4 and 6 mm. In figure 4 we present averaged electric field and electron density profiles at various times. In figure 5, a 3D view of the electron density at 4.05 ns is shown. The

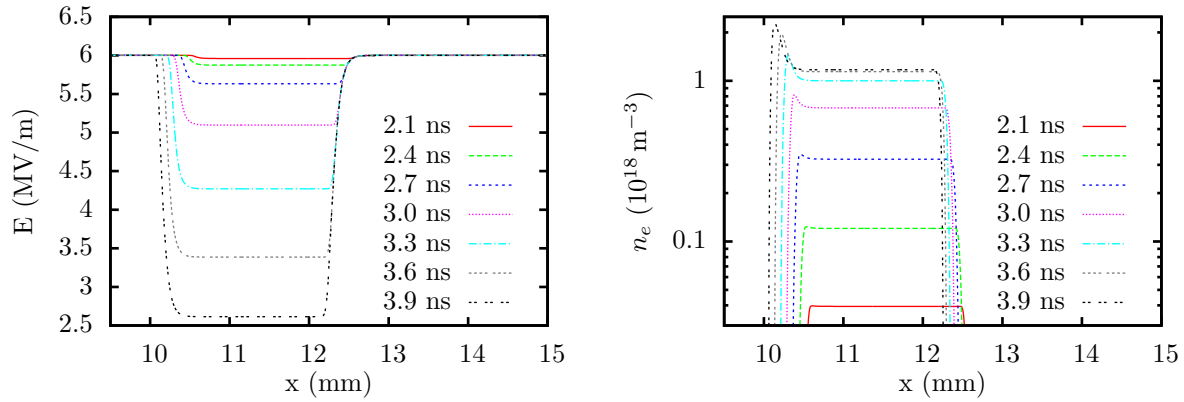


Figure 3. Partial screening of the electric field in the 1D fluid simulations, for a background field of 6 MV/m and an initial plasma density of 10^{13} m^{-3} . The electric field (left) and the electron density (right) are shown at various times. The exponential growth of the electron density slows down because the electric field gets screened.

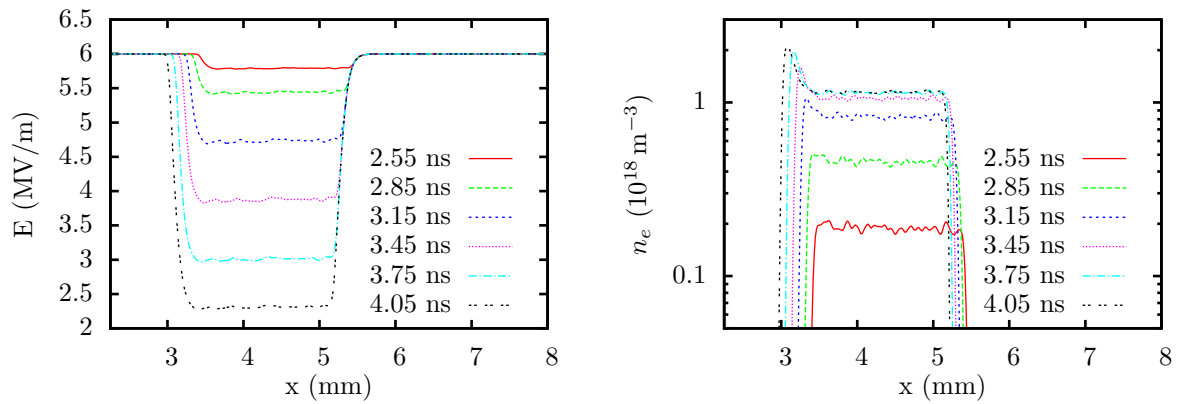


Figure 4. Electric field and electron density in the 3D particle simulations, for a background field of 6 MV/m and an initial density of $n_0 = 10^{13} \text{ m}^{-3}$. The values are averaged over planes perpendicular to the x -direction.

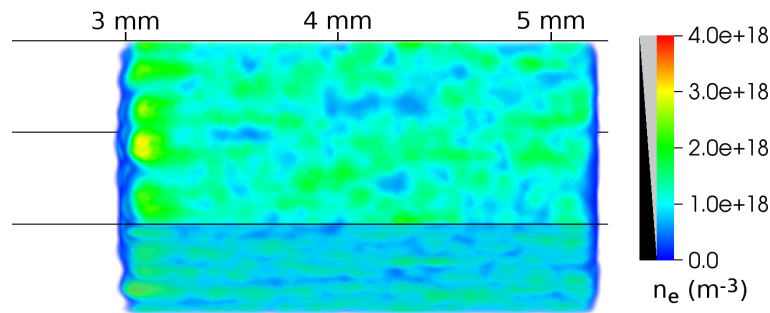


Figure 5. The electron density in the 3D particle model at 4.05 ns, for an initial density of $n_0 = 10^{13} \text{ m}^{-3}$. (This figure is made using volume rendering; transparency is indicated in the legend.)

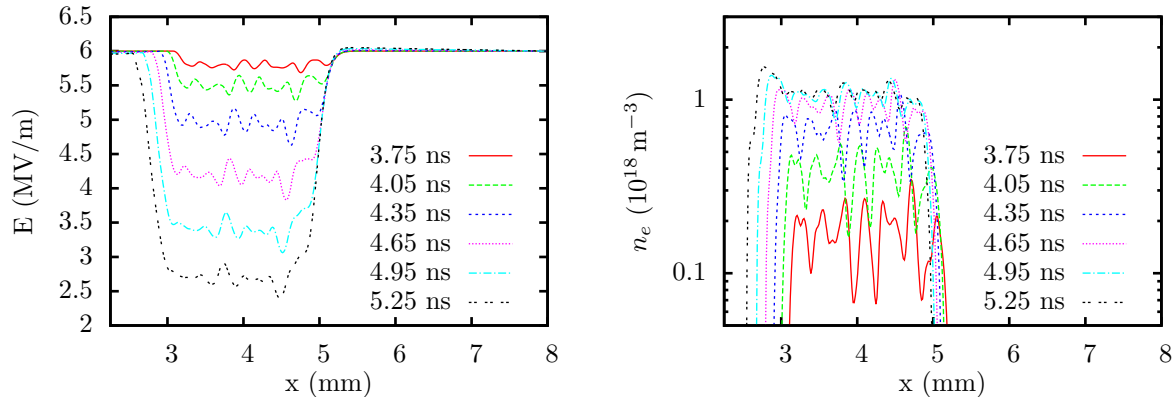


Figure 6. Electric field and electron density in the 3D particle simulations, as in figure 4, but now for a lower initial density of $n_0 = 10^{11} \text{ m}^{-3}$.

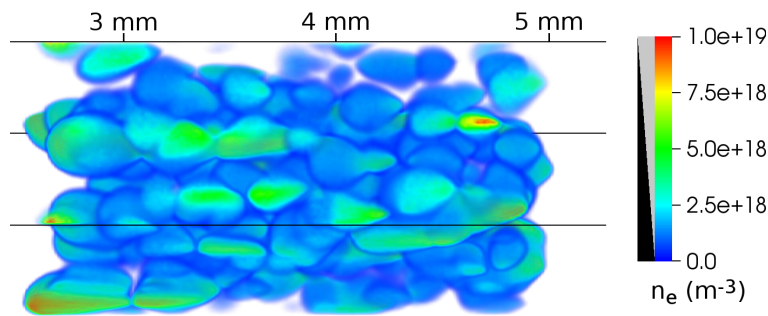


Figure 7. The electron density in the 3D particle model at 5.25 ns, for an initial density of $n_0 = 10^{11} \text{ m}^{-3}$.

screening time is about 3.75 ns, as in the 1D case of figure 3. Some noise can be seen in the electric field and density profiles, because the initial density corresponds to 10^4 electrons per mm^3 .

With an initial density of $n_0 = 10^{11} \text{ m}^{-3}$, the results look quite different, see figures 6 and 7. There is now significant noise in the electric field and especially in the electron density profiles. These larger fluctuations emerge because the initial density corresponds to only 10^2 electrons per mm^3 . The screening time is about 5.1 ns, which is still in agreement with the 1D results of figure 2.

Compared to the 1D results, we observe almost the same screening times in 3D, but with lower initial densities fluctuations become larger. If we would further reduce the initial electron density, we would eventually get a few separated electron avalanches that develop into streamers.

4. The homogeneity of discharges

In the previous section we have seen that discharges can develop quite irregularly if the initial electron density is low. The irregularities cause field enhancement, that could invalidate our estimate for the ionization screening time. To estimate when this happens,

we first discuss how long it takes for space charge effects to develop.

4.1. The streamer formation time

If an electron avalanche starts from a single electron, how long does it take for space charge effects to become significant? In other words, how long does it take for a streamer to form? The answer depends on the processes that can affect the space charge fields: ionization, drift and diffusion. The coefficients of these processes can be described in terms of the electric field E and the gas number density N , so that in general the ‘streamer formation time’ is a function of E and N . According to [11, 12], the number of electrons required for a streamer to form scales as $g(E) \cdot N_0/N$, where $g(E)$ is some function of the electric field and N_0 is the density of air at standard temperature and pressure. Then the time scale for streamer formation can be expressed as

$$\tau_{\text{streamer}} = \ln [g(E) \cdot N_0/N] / (\alpha_{\text{eff}} v_d).$$

For $N = N_0$, a commonly used empirical approximation is to take $g(E) \approx 10^8$, so that $\ln[g(E)] \approx 18$. This criterion is known as the Raether-Meek criterion, for which the streamer formation time is given by

$$\tau_{\text{RM}} \approx 18 / (\alpha_{\text{eff}} v_d). \quad (10)$$

4.2. Required pre-ionization for homogeneity

From the previous section we have an estimate for the time it takes to develop space charge effects. Given this time, we can estimate how high the initial electron density n_0 needs to be to prevent streamer formation. Several authors have made such estimates in the past, see for example [13, 14, 15]. Much of this research was aimed at generating homogeneous discharges for CO₂ lasers. Below, we derive an alternative criterion for homogeneity that is based on arguments from [13, 14, 15], but perhaps simpler.

As long as space charge effects are negligible, the electron avalanche will radially expand due to diffusion. In the radial direction, the electron density at time t will have a Gaussian distribution with a standard deviation of $\sqrt{2D_e t}$. If we let R_s denote the typical radius at the time of streamer formation, see equation (10), we get $R_s = 6\sqrt{D_e/(v_d\alpha)}$. If streamer formation is to be prevented, the avalanches need to be sufficiently close to each other. This means that their initial separation should be on the order of R_s . Suppose it is $k \cdot R_s$, where k is about one, then the initial electron density n_0 should be at least

$$n_0 \approx 1/(R_s)^3 = \frac{1}{216k^3} \left(\frac{v_d\alpha}{D_e} \right)^{3/2}. \quad (11)$$

In figure 8, equation (11) is shown against the electric field for N₂ at 1 bar, for three values of k . We can see that the result is quite sensitive to k . Using $1 \leq k \leq 3$, the required initial density lies between 10^{12} and 10^{13} m^{-3} for a field of 6 MV/m, in agreement with the results from section 3.3.

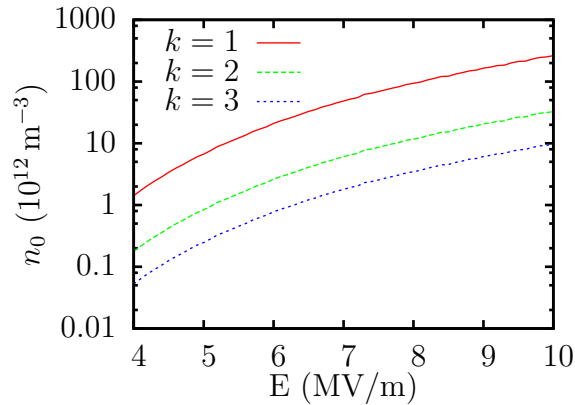


Figure 8. The required initial electron density for homogeneous breakdown according to equation (11), for three values of k . The curves shown are for N_2 at 1 bar.

5. The effect of detachment and photoionization

Besides impact ionization, there can be other ways to generate free electrons in a gas, which may affect our estimate for the screening time. This is especially true for air, in which electron detachment and photoionization can occur. The effect of these processes is discussed below.

5.1. Electron detachment

In electronegative gases there might initially be negative ions instead of free electrons. Ionization screening by electrons can still take place in such a gas if electrons are able to detach from the negative ions. If a typical time scale for detachment is τ_d , then the screening process will be delayed by approximately

$$\tau_{\text{delay}} = \ln(1 + \tau_d \alpha_{\text{eff}} v_d) / (\alpha_{\text{eff}} v_d), \quad (12)$$

so that the total screening time is given by the sum of equations (6) and (12)

$$\tau_{\text{is}} = \left[\ln \left(1 + \frac{\alpha_{\text{eff}} \varepsilon_0 E_0}{e n^-} \right) + \ln(1 + \tau_d \alpha_{\text{eff}} v_d) \right] / (\alpha_{\text{eff}} v_d), \quad (13)$$

where n^- denotes the negative ion density. Equation (12) is the solution to $n_e(\tau_{\text{delay}}) = n^-$ given the following equation

$$\partial_t n_e(t) = n^- / \tau_d + n_e(t) \alpha_{\text{eff}} v_d,$$

with $n_e(0) = 0$. This last equation describes the growth of the electron density in time, but it does not take the depletion of negative ions by detachment into account (n^- should change in time). The underlying assumption is that ionization quickly dominates over detachment. Furthermore, the coefficients τ_d , α_{eff} and v_d are assumed to be constant, since we do not expect the electric field to change during the detachment phase.

Summarizing, if there are negative ions from which electrons first have to detach, then there will be a delay in the ionization screening process. The ionization screening time can then be approximated by equation (13).

5.2. Photoionization

Photoionization can occur if excited molecules (or atoms) emit photons energetic enough to ionize other molecules (or atoms). With a few assumptions, we can estimate how photoionization will affect the screening time. Suppose that on average η photoionization events take place per electron-impact ionization. Suppose further that these photoionizations take place at a distance that is larger than $n_0^{-1/3}$, where n_0 is the initial density of electrons. If there is no delay in emitting the ionizing photons, and if space charge effects can be neglected, then the electron density will grow as

$$n_e(t) = n_0 e^{(1+\eta)\alpha_{\text{eff}}v_d t}. \quad (14)$$

So, photoionization effectively increases α_{eff} with a factor $1 + \eta$. For air at atmospheric pressure η is less than 1%, and at low pressures $\eta \lesssim 0.1$ [16]. Therefore photoionization does not change the ionization screening time (6) much.

Another effect of photoionization could be to make a discharge more homogeneous. One interpretation of equation (14) is that photoionization has effectively increased the initial density n_0 by a factor $e^{\eta\alpha_{\text{eff}}v_d t}$ at time t . From equation (10), we get that $\alpha_{\text{eff}}v_d t \approx 18$ when space charge effects set in. For $\eta = 1\%$, the factor $e^{18\eta}$ is about 1.2, so that the effect of photoionization on the homogeneity of a discharge is rather weak. For $\eta \approx 0.1$, the factor is about 6, so that photoionization should be taken into account.

6. Conclusion

We have introduced the ionization screening time, a generalization of the Maxwell time that is also valid for electric fields above breakdown. An analytic estimate for this time scale was introduced, which was compared with numerical simulations in 1D and 3D, finding good agreement. We have given an estimate for the required plasma density to prevent the growth of inhomogeneities, and we have discussed the effects of electron detachment and photoionization on ionization screening.

These results can help to understand the development of pulsed discharges, such as nanosecond pulsed discharges at atmospheric pressure or halo discharges in the lower ionosphere. First, our estimate can be used to predict whether such a discharge initially develops homogeneously. If so, then two stages can be distinguished: Before the ionization screening time, growth takes place in the complete discharge volume. After this time, the discharge grows at its boundary, because its interior is electrically screened.

Acknowledgments

JT was supported by STW project 10755. ABS acknowledges the support by an NWO Valorization project at CWI and by STW projects 10118 and 12119.

References

- [1] Michael S. Barnes, Tina J. Cotler, and Michael E. Elta. Large-signal time-domain modeling of low-pressure rf glow discharges. *Journal of Applied Physics*, 61(1):81, 1987.
- [2] A. B. Sun, J. Teunissen, and U. Ebert. Why isolated streamer discharges hardly exist above the breakdown field in atmospheric air. *Geophys. Res. Lett.*, 40(10):24172422, May 2013.
- [3] A. B. Sun, J. Teunissen, and U. Ebert. The inception of pulsed discharges in air: simulations in background fields above and below breakdown. Submitted to *J. Phys. D: Appl. Phys.*
- [4] Alejandro Luque and Ute Ebert. Emergence of sprite streamers from screening-ionization waves in the lower ionosphere. *Nature Geoscience*, 2(11):757760, Nov 2009.
- [5] S.T. Surzhikov. *Computational Physics of Electric Discharges in Gas Flows*. De Gruyter Studies in Mathematical Physics. De Gruyter, 2012.
- [6] C. Montijn, W. Hundsdorfer, and U. Ebert. An adaptive grid refinement strategy for the simulation of negative streamers. *Journal of Computational Physics*, 219(2):801835, Dec 2006.
- [7] Siglo database, retrieved april 2013.
- [8] Z.M. Rospopovic, S. Sakadzic, S.A. Bzenic, and Z.Lj. Petrovic. Benchmark calculations for monte carlo simulations of electron transport. *IEEE Trans. Plasma Sci.*, 27(5):12411248, 1999.
- [9] J. Adams, P. Swarztrauber, and R. Sweet. Fishpack90, <http://www.cisl.ucar.edu/css/software/fishpack90>, 2011.
- [10] Jannis Teunissen and Ute Ebert. Controlling the weights of simulation particles: adaptive particle management using k-d trees. *Journal of Computational Physics*, 259:318330, Feb 2014.
- [11] Carolynne Montijn and Ute Ebert. Diffusion correction to the raethermcek criterion for the avalanche-to-streamer transition. *J. Phys. D: Appl. Phys.*, 39(14):29792992, Jul 2006.
- [12] Ute Ebert, Sander Nijdam, Chao Li, Alejandro Luque, Tanja Briels, and Eddie van Veldhuizen. Review of recent results on streamer discharges and discussion of their relevance for sprites and lightning. *Journal of Geophysical Research*, 115, 2010.
- [13] A. Jay Palmer. A physical model on the initiation of atmospheric-pressure glow discharges. *Appl. Phys. Lett.*, 25(3):138, 1974.
- [14] Jeffrey I. Levatter and Shao-Chi Lin. Necessary conditions for the homogeneous formation of pulsed avalanche discharges at high gas pressures. *Journal of Applied Physics*, 51(1):210, 1980.
- [15] G. Herziger, R. Wollermann-Windgasse, and K. H. Banse. On the homogeneization of transverse gas discharges by preionization. *Appl. Phys.*, 24(3):267272, Mar 1981.
- [16] M. B. Zhelezniak, A. K. Mnatsakanian, and S. V. Sizykh. Photoionization of nitrogen and oxygen mixtures by radiation from a gas discharge. *Teplofizika Vysokikh Temperatur*, 20:423–428, Nov 1982.